Microstructures to Control Elasticity in 3D Printing – Supplemental Material

Christian Schumacher[1,2] Bernd Bickel[1,3] Jan Rys[2] Steve Marschner[4] Chiara Daraio[2] Markus Gross[1,2]

[1]Disney Research Zurich [2]ETH Zurich [3]IST Austria [4]Cornell University

1 Numerical Coarsening

We use a homogenization method to describe the coarse-scale behavior of a microstructure, and as the basis of our microstructure optimization. Such a method computes material parameters for a homogenous material that approximates a structure. In the following, we summarize the *Numerical Coarsening* approach [Kharevych et al. 2009] and highlight differences due to its application to microstructures.

Harmonic Displacements To describe the deformation behavior of the microstructure, a set of representative displacements have to be computed for different load cases. These *harmonic displacements* $\mathbf{h}_{ab}$ (see Figure 1 for an illustration) are defined as the solution to the following boundary value problem:

$$\begin{aligned} \nabla \cdot \boldsymbol{\sigma}(\mathbf{h}_{ab}) &= 0 && \text{inside } \Omega \\ \boldsymbol{\sigma}(\mathbf{h}_{ab}) \cdot \mathbf{n} &= \tfrac{1}{2}(\mathbf{e}_a \mathbf{e}_b^T + \mathbf{e}_b \mathbf{e}_a^T) \cdot \mathbf{n} && \text{on } \partial\Omega. \end{aligned} \tag{1}$$

Here, $\mathbf{e}_a$ is the unit vector along the a-th coordinate direction, $\frac{1}{2}(\mathbf{e}_a \mathbf{e}_b^T + \mathbf{e}_b \mathbf{e}_a^T)$ describes the tractions on the surface $\partial\Omega$ of the object domain Ω, and $\mathbf{n}$ is the surface normal. For tiled structures, this surface is the boundary of the cell.

Considering symmetries, there are 3 and 6 distinct harmonic displacements in 2D and 3D, respectively. From these displacements, a 4-th order deformation tensor $\mathbf{G}$ can be defined per element:

$$\mathbf{G}_{klab} = \left(\boldsymbol{\varepsilon}\left(\mathbf{h}_{ab}\right)\right)_{kl}. \tag{2}$$

This tensor contains the Cauchy strain for every displacement, and by considering the elasticity equation $W = \boldsymbol{\varepsilon} : \mathbf{C} : \boldsymbol{\varepsilon}$ as a bilinear equation, the term $\mathbf{G}^T : \mathbf{C} : \mathbf{G}$ describes the energy density for any pair of harmonic displacements.

Coarsening The homogenized material stiffness tensor can then be computed from the deformation behavior of the microstructure. The deformation is first transferred from the harmonic displacements of the microstructure to a coarse mesh consisting of only a single voxel of the size of the cell. For the case where the corners of the cell correspond to vertices of the fine mesh, this simply means transferring the displacements at the corner. For the general case, the displacement is transferred by computing a distance-weighted interpolation of a set of nearest neighbors in the fine mesh, while adhering to the periodic boundary conditions. After the deformation has been transferred to the coarse mesh, a single coarse-scale deformation tensor $\mathbb{G}$ can be defined in a manner similar to Equation (2). The coarsened material stiffness tensor for the coarse mesh is then obtained analytically as

$$\mathbb{C} = \mathbb{G}^{-T} : \left(\sum_{i=1}^{k} \frac{V_i}{V} \mathbf{G}_i^T : \mathbf{C}_i : \mathbf{G}_i \right) : \mathbb{G}^{-1}, \tag{3}$$

where in the 2D (3D) case V_i is the area (volume) of element i in the fine mesh, and V is the area (volume) of the entire cell. This approach differs slightly from Kharevych et al. [2009], where a coarsened material stiffness tensor is computed for every element in a coarse tetrahedral mesh. Due to the periodic boundary condition for microstructures, the strain in the coarse mesh is uniform, and a single material stiffness tensor can be computed for the whole cell. Note that we use the Voigt compressed matrix representation to express all tensors. This is especially important when computing $\mathbb{G}^{-1}$, which can be computed as a simple matrix inverse instead of a more complex symmetric tensor inverse.

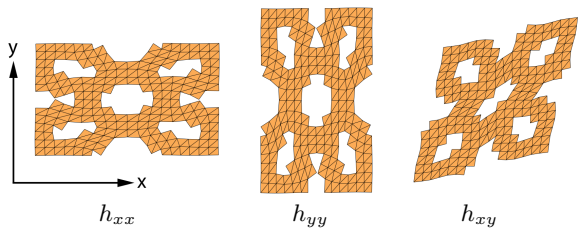

Figure 1: *Harmonic displacements of a microstructure cell in 2D.*

2 Microstructure Optimization in 3D

This section describes the changes necessary to transform the microstructure optimization described in Section 5 of the paper from 2D to 3D.

2.1 Regularization

Two of the regularization terms, the smoothness term and the checkerboard term, rely on neighborhood information and have to be adapted accordingly in a 3D environment.

Smoothness The approach for the smoothness term in 3D is identical to the 2D case, except that we now use six neighbors instead of four to compute the second-order finite difference approximation. Assuming each component of $\boldsymbol{\alpha}$ is associated with three indices in 3D, such that $\boldsymbol{\alpha}_{i,j,k}$ corresponds to the voxel (i, j, k), the regularization has the form

$$\begin{aligned} R_s = \sum_{i,j,k} (&\boldsymbol{\alpha}_{i-1,j,k} + \boldsymbol{\alpha}_{i+1,j,k} + \boldsymbol{\alpha}_{i,j-1,k} \\ &+ \boldsymbol{\alpha}_{i,j+1,k} + \boldsymbol{\alpha}_{i,j,k-1} + \boldsymbol{\alpha}_{i,j,k+1} \\ &- 6\boldsymbol{\alpha}_{i,j,k})^2 \end{aligned} \tag{4}$$

Checkerboard patterns In 3D, checkerboard patterns include structures that are connected by a single vertex or a single edge. To cover these two cases, we will split the regularization term in two components, $R_{cb,v}$ and $R_{cb,e}$, respectively.

To check for structures connected by a single vertex, $R_{cb,v}$ has to cover patches of $2 \times 2 \times 2$ voxels. For these patches, there are four configurations that are undesirable and will not be covered by $R_{cb,e}$. These are the only configurations for which a binary solution

should lead to a regularization value larger than 0. This condition can be formulated as

$$
\begin{aligned}
R_{cb,e} = \sum_{i,j,k} & (\boldsymbol{\alpha}_{i,j,k} - \boldsymbol{\alpha}_{min})(1 - \boldsymbol{\alpha}_{i+1,j,k}) \\
& (1 - \boldsymbol{\alpha}_{i,j+1,k})(1 - \boldsymbol{\alpha}_{i,j,k+1}) \\
& (1 - \boldsymbol{\alpha}_{i+1,j+1,k})(1 - \boldsymbol{\alpha}_{i+1,j,k+1}) \\
& (1 - \boldsymbol{\alpha}_{i,j+1,k+1})(\boldsymbol{\alpha}_{i+1,j+1,k+1} - \boldsymbol{\alpha}_{min}) \\
& +(1 - \boldsymbol{\alpha}_{i,j,k})(\boldsymbol{\alpha}_{i+1,j,k} - \boldsymbol{\alpha}_{min}) \\
& (1 - \boldsymbol{\alpha}_{i,j+1,k})(1 - \boldsymbol{\alpha}_{i,j,k+1}) \\
& (1 - \boldsymbol{\alpha}_{i+1,j+1,k})(1 - \boldsymbol{\alpha}_{i+1,j,k+1}) \\
& (\boldsymbol{\alpha}_{i,j+1,k+1} - \boldsymbol{\alpha}_{min})(1 - \boldsymbol{\alpha}_{i+1,j+1,k+1}) \\
& +(1 - \boldsymbol{\alpha}_{i,j,k})(1 - \boldsymbol{\alpha}_{i+1,j,k}) \\
& (\boldsymbol{\alpha}_{i,j+1,k} - \boldsymbol{\alpha}_{min})(1 - \boldsymbol{\alpha}_{i,j,k+1}) \\
& (1 - \boldsymbol{\alpha}_{i+1,j+1,k})(\boldsymbol{\alpha}_{i+1,j,k+1} - \boldsymbol{\alpha}_{min}) \\
& (1 - \boldsymbol{\alpha}_{i,j+1,k+1})(1 - \boldsymbol{\alpha}_{i+1,j+1,k+1}) \\
& +(1 - \boldsymbol{\alpha}_{i,j,k})(1 - \boldsymbol{\alpha}_{i+1,j,k}) \\
& (1 - \boldsymbol{\alpha}_{i,j+1,k})(\boldsymbol{\alpha}_{i,j,k+1} - \boldsymbol{\alpha}_{min}) \\
& (\boldsymbol{\alpha}_{i+1,j+1,k} - \boldsymbol{\alpha}_{min})(1 - \boldsymbol{\alpha}_{i+1,j,k+1}) \\
& (1 - \boldsymbol{\alpha}_{i,j+1,k+1})(1 - \boldsymbol{\alpha}_{i+1,j+1,k+1})
\end{aligned}
\tag{5}
$$

Structures that are connected by a single edge can be detected by looking at patches of $2 \times 2 \times 1$ voxels, similar to the regularization in 2D. The only

$$
\begin{aligned}
R_{cb,v} = \sum_{i,j,k} & (1 - \boldsymbol{\alpha}_{i,j,k})(\boldsymbol{\alpha}_{i+1,j,k} - \boldsymbol{\alpha}_{min}) \\
& (\boldsymbol{\alpha}_{i,j+1,k} - \boldsymbol{\alpha}_{min})(1 - \boldsymbol{\alpha}_{i+1,j+1,k}) \\
& +(\boldsymbol{\alpha}_{i,j,k} - \boldsymbol{\alpha}_{min})(1 - \boldsymbol{\alpha}_{i+1,j,k}) \\
& (1 - \boldsymbol{\alpha}_{i,j+1,k})(\boldsymbol{\alpha}_{i+1,j+1,k} - \boldsymbol{\alpha}_{min}) \\
& +(1 - \boldsymbol{\alpha}_{i,j,k})(\boldsymbol{\alpha}_{i+1,j,k} - \boldsymbol{\alpha}_{min}) \\
& (\boldsymbol{\alpha}_{i,j,k+1} - \boldsymbol{\alpha}_{min})(1 - \boldsymbol{\alpha}_{i+1,j,k+1}) \\
& +(\boldsymbol{\alpha}_{i,j,k} - \boldsymbol{\alpha}_{min})(1 - \boldsymbol{\alpha}_{i+1,j,k}) \\
& (1 - \boldsymbol{\alpha}_{i,j,k+1})(\boldsymbol{\alpha}_{i+1,j,k+1} - \boldsymbol{\alpha}_{min}) \\
& +(1 - \boldsymbol{\alpha}_{i,j,k})(\boldsymbol{\alpha}_{i,j+1,k} - \boldsymbol{\alpha}_{min}) \\
& (\boldsymbol{\alpha}_{i,j,k+1} - \boldsymbol{\alpha}_{min})(1 - \boldsymbol{\alpha}_{i,j+1,k+1}) \\
& +(\boldsymbol{\alpha}_{i,j,k} - \boldsymbol{\alpha}_{min})(1 - \boldsymbol{\alpha}_{i,j+1,k}) \\
& (1 - \boldsymbol{\alpha}_{i,j,k+1})(\boldsymbol{\alpha}_{i,j+1,k+1} - \boldsymbol{\alpha}_{min})
\end{aligned}
\tag{6}
$$

3 Numerical Methods

The indirect relationship between the coarsened stiffness tensor $\mathbb{C}(h(\boldsymbol{\alpha}))$ and the activations $\boldsymbol{\alpha}$ through the harmonic displacements $\mathbf{h}(\boldsymbol{\alpha})$ defined in Equation (1) has to be taken into account when computing the derivatives of the microstructure optimization problem introduced in the paper. When the chain rule is applied to this problem, the Jacobian of the harmonic displacements with respect to the activations emerges. Since these quantities are effectively linked by the solution of an elasticity problem, given the boundary tractions defined in (1), we use the adjoint method to compute the Jacobian. For this, we take the derivatives of both the minimization condition $\nabla_{\mathbf{x}} U_{el} = 0$ and the constraints $\mathbf{c} = 0$ with respect to $\boldsymbol{\alpha}$:

$$
\begin{aligned}
\frac{\partial^2 U_{el}}{\partial \mathbf{h}_{ab}\, \partial \boldsymbol{\alpha}} + \frac{\partial^2 U_{el}}{\partial {\mathbf{h}_{ab}}^2} \frac{d\mathbf{h}_{ab}}{d\boldsymbol{\alpha}} &= 0 \\
\frac{\partial \mathbf{c}}{\partial \mathbf{h}_{ab}} \frac{d\mathbf{h}_{ab}}{d\boldsymbol{\alpha}} &= 0.
\end{aligned}
\tag{7}
$$

Solving this system of equations for the desired Jacobian ${}^{d\mathbf{h}_{ab}}/_{d\boldsymbol{\alpha}}$ requires only a single sparse matrix decomposition.

4 Compression Test Data

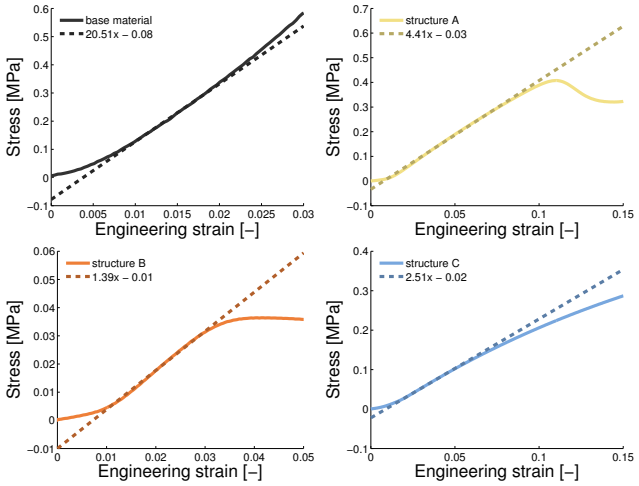

Figure 2: *The stress–strain measurements for the base material and the three structures tested in the compression test. The tangents of the linear part of the curve describes the Young's modulus of the structure.*

Figure 2 shows the data from the compression tests of the base material and three synthesized structure. We determined the Young's modulus of the structures by fitting a linear polynomial to the linear part of the stress–strain curve.

References

KHAREVYCH, L., MULLEN, P., OWHADI, H., AND DESBRUN, M. 2009. Numerical coarsening of inhomogeneous elastic materials. *ACM Trans. Graph. (Proc. SIGGRAPH) 28*, 51.